Proc. Indian Acad. Sci. (*Chem. Sci.*), Vol. 115, No. 2, April 2003, pp 91–102

Synthesis and room temperature single crystal EPR studies of a dinickel complex having an $\{Ni_2(m\text{-phenoxide})_2\}^{2+}$ unit supported by a macrocyclic ligand environment $[Ni_2(L)_2(OClO_3)_2]$ [L = 2-[(4-methyl-pyridin-2-ylimino)-methyl]-phenol]

R SRINIVASAN, I SOUGANDI, R VENKATESAN and
P SAMBASIVA RAO*
Department of Chemistry, Pondicherry University, Pondicherry 605 014, India
e-mail: psr52in@yahoo.co.in

MS received 17 October 2002; revised 11 March 2003

Abstract. A bimetallic nickel(II) complex with the ligand Hsalamp (2-[(4-methyl-pyridin-2-ylimino)-methyl]-phenol), having the molecular formula, $Ni_2C_{26}H_{22}N_4O_{10}Cl_2$, is synthesized and characterized by elemental, UV-Vis, IR and EPR studies. The IR spectrum confirms the presence of coordinated perchlorate ion and the UV-Vis. spectrum substantiates that the geometry around the metal ion is distorted square pyramidal. In the solvent methanol, the complex undergoes dissociation indicating the nature of the complex to be 1 : 2 electrolyte. The single crystal EPR studies indicate that the zero-field splitting is not large and the spectra can be observed even at room temperature, not so common for a nickel(II) ion. The spin Hamiltonian parameters calculated from single crystal rotations are: g – 2·377, 2·219, 2·071 and D – 9·7, 4·2 and – 13·9 mT. Optical and electron paramagnetic spectral data have been used to obtain the parameters *Dq*, *B* and *C*.

Keywords. Hsalamp; cyclic voltammetry; electron paramagnetic resonance; spin-Hamiltonian parameters.

1. Introduction

Biological activity of complexes derived from hydrazones has been widely studied and contrasted, acting in processes such as antibacterial, antitumoral, antiviral, antimalarial and antituberculosis effects.[1] The antitumoural and antiviral activities of many complexes derived from hydrazones such as thiosemicarbazones have also been reported.[2–5] Often these compounds show an N,N,S-coordinating pattern; however, there is very little information about O,N,O- or N,N,O-coordinated hydrazone compounds in the literature. Potentially pentadentate ligands $SalXH_2$(1) have been prepared by the Schiff's base condensation of salicylaldehyde with tridentate amines. Single crystal X-ray diffraction studies on two nickel complexes with SalX ligands (X = NH, NCH_3) have shown the metal environments to be intermediate between square pyramidal and trigonal-bipyramidal geometries,[6,7] while other studies have shown that Zn(cbpN).H_2O,

*For correspondence

Zn(mbpN).H_2O, Ni(mbpN) and Cu(mbpN) are all five-coordinate with the central donor atom coordinated to the metal atom.[8,9] The zinc complexes have trigonal bipyramidal geometry, while the copper and nickel complexes have distorted square pyramidal geometry.

Hence, in this communication, we describe the synthesis of a nickel complex with the ligand, 2-[(4-methyl-pyridin-2-ylimino)-methyl]-phenol (Hsalamp). The complex is characterized mainly by UV-Vis, IR and EPR techniques. The results indicate that the complex is dimeric in nature, with perchlorate coordination within the coordination sphere and the EPR spectrum shows no half-field transitions, confirming non-interaction between the two metal ions.

Nickel(II) (d^8) ion being a non-Krammer's ion, EPR spectra is observable, generally at low temperatures. However, there are very few reports in the literature about the study of this d^8 ion at room temperature. Most of the reported work concerns the study of this ion at 77 K or 4 K.[10–22] The g value is isotropic and close to 2·2. In general, if the zero-field splitting (D) is negligible, one would expect and observe a single EPR line. However, in most of the systems, D is non-zero and hence more than one line has been observed. In a recently communicated paper dealing with nickel(II) doped in hexaimidazole zinc(II)dichloride tetrahydrate,[23] we have observed a maximum of two resonance lines, which completely merge to a single line or sometimes go out of the reach of our X-band magnetic field region, during crystal rotations. Hence, it has been concluded that the system has a large zero-field splitting, compared to X-band energy. There are a few extra resonance lines, which might have been arisen from forbidden transitions. Generally, when zero-field splitting is large, one would expect forbidden transitions.[22] The EPR spectral parameters of nickel(II) in $[Ni(C_3H_4N_2)_6](NO_3)_2$ having trigonal symmetry are determined from powder and single crystal measurements[10] as $g = 2{\cdot}185$, $D = 0{\cdot}882$ cm^{-1}, $E = 0$. Single-ion spin Hamiltonian parameters are determined for zinc fluoroborate hexahydrate doped with nickel(II) and compared with those obtained for the nickel fluoroborate hexahydrate.[11] EPR studies are carried out for several concentrations ($x = 0{\cdot}005$ to 1) from room to liquid helium temperatures. However, for temperatures between 4·2 and 1·5 K and for low doping, the parameters are constant with $g_{\|} = 2{\cdot}229$, $g_{\perp} = 2{\cdot}261$ and $D = -0{\cdot}1219$ cm^{-1}. In contrast, for nickelfluoroborate, the values are the same, with weak temperature dependence, attributed to ferromagnetic interaction. At high temperature, these parameters are remar kably concentration-dependent. The study of line width dependence as a function of concentration has indicated that the nickel(II) ions have randomly occupied zinc sites. The d^8 ion in trigonal field is studied very extensively using Al_2O_3[24,25] as the host lattice and the calculated $g_{\|}$, $g_{\perp}$ and D values are 2·1948(10), 2·1853(10) and $-1{\cdot}312$ mT respectively. Single crystal EPR studies of nickel(II) in hexakis(pyrazole) complexes of zinc(II) and cadmium(II) are reported.[26] Nickel(II) is used to study phase transitions in $RbCaF_3$ single crystals at 25 K.[27]

2. Experimental

2.1 *Physical measurements*

IR spectra of the ligands and complexes are recorded using a Jasco FT-IR-5300 instrument (KBr pellet technique) in the region 500–4000 cm^{-1}. UV-Vis spectra are obtained using a Milton Roy Spectronic 1201 spectrophotometer with a quartz cell. The ^{1}H NMR spectrum of the ligand is obtained in $CDCl_3$ with TMS as the internal reference,

on a 300 MHz Bruker AMX-Spectrometer. EPR spectra are recorded using a JEOL JES-TE100 ESR spectrometer operating at X-band frequencies and having a 100 kHz modulation to obtain first derivative EPR signal. Single crystals are mounted on a goniometer for crystal rotations and the spectra are recorded for every 10° orientations of the external magnetic field about the three mutually orthogonal axes. The powdered samples are placed in a quartz tube for EPR measurements.

2.2 *Materials*

Tetrabutylammonium perchlorate [TBAP], used as the supporting electrolyte in electrochemical measurements, was obtained from Fluka and recrystallized from water. Acetonitrile (AR grade) was obtained from BDH. All other chemicals and solvents of reagent grade were used as received.

2.3 *Preparation of ligand*

The Schiff's base ligand, 2-[(4-methyl-pyridin-2-ylimino)-methyl]-phenol, abbreviated as Hsalamp, is prepared by the condensation of 4-methyl-2-aminopyridine with salicyl-aldehyde in 1 : 1 ratio in pure dry ethanol. Dark yellow diamond-shaped crystals of the ligand, obtained after the evaporation of the solvent, are characterized by elemental analysis, IR, UV-Vis, NMR and mass techniques. IR spectra reveal C=N stretching at 1597·.2 cm^{-1}. ^1H NMR, elemental and mass spectral data are also in good agreement with the expected structure.

2.4 *Preparation of the complex*

The nickel complex is prepared by taking two equivalents of the ligand (2·12 g, 0·01 moles) with two equivalent of nickel perchlorate (3·6571 g, 0·01 moles) in dry methanol. Initially, the ligand Hsalamp is first dissolved in methanol, where the colour of the solution is yellow. To this, methanolic solution of nickel perchlorate is added, wherein change in colour is observed from yellow to light green. The whole solution is then kept under reflux for 8 h (around 300 K). Slow evaporation of this solution results in the formation of a pale greenish-yellow coloured powder. Scheme 1 gives a systematic procedure for the preparation of the nickel complex, the structure of which is confirmed by EPR studies.

Analytical data for the complex are as follows: Molecular formula of $Ni_2C_{26}H_{22}N_4O_{10}Cl_2$, calculated (found): C = 42·2 (42·1), H = 2·98 (2·9), N = 7·5 (7·5), Ni = 15·9 (15·8)%. Agreement between calculated and experimental values is thus very good, confirming the formation of the complex with the mentioned molecular formula. The melting of the complex is determined as 385 K.

3. Results and discussion

3.1 *IR studies*

The IR spectrum of the nickel complex shows a peak in the region 1439 cm^{-1}, assigned to the stretching vibrations of the aromatic skeleton.[28] As mentioned earlier,[29] the peaks around 1150, 1093 and 621 cm^{-1} ($n(ClO_4)$), confirm the presence of a coordinated perchlorate ion. The C=N stretching frequency observed at about 1607 cm^{-1} establishes

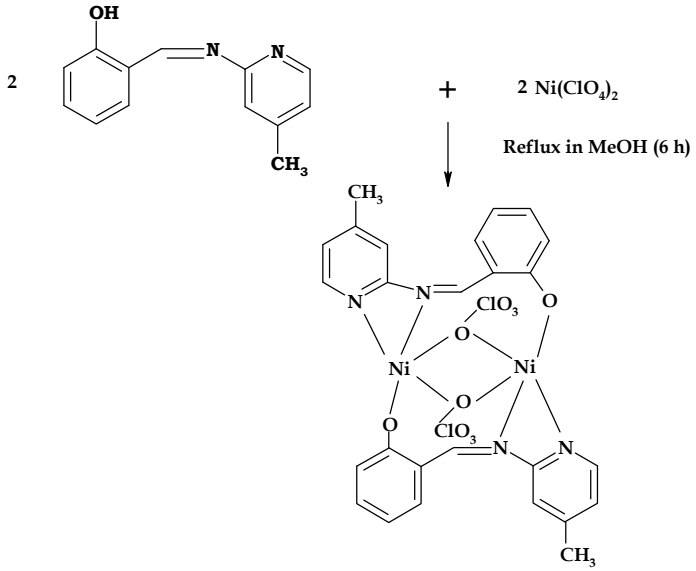

Scheme 1.

the participation of nitrogen in the complex formation.[28] Shifting of frequencies between the pure ligand and complex is noticed, confirming the formation of the complex.

The molar conductance for the complex measured in MeOH solvent is 230 *l*m/S cm^2 mol^{-1}, which indicates that the complex is ionic and bivalent type. Observing a molar conductance of 225 *l*mS cm^2 mol^{-1}, confirms the charge of the complex is +2, as reported earlier.[30] In the solvent, the complex undergoes dissociation indicating the nature of the complex to be 1 : 2 electrolyte.[31]

3.2 *Optical studies*

The electronic spectrum of the nickel complex, recorded in methanol solvent, contains *d*–*d* bands at 998, 660, a shoulder at 720 and a charge transfer band at 400 nm (figure 1). Calculated absorbance values are 9340, 15290 and 22020 (e/mol^{-1} cm^{-1} dm^3). It is reported that in the visible–near-infrared spectra of nickel complexes in CH_2Cl_2 solvent, bands observed around 1150, 950 and 600 nm confirm that the geometry around the metal ion is distorted square pyramidal.[32,33] However, for nickel(II) complexes having six imidazole units, in a nearly octahedral fashion, three strong bands and a weak band a re reported at 957, 591, 365 and 731 nm respectively.[23]

A detailed understanding of paramagnetic resonance spectra requires the knowledge of the position of the excited levels, for the ground state is always a pure state. Nickel(II) ion (d^8) gives rise to the free ion terms ^3F, ^3P, ^1D, ^1G and ^1S, the ground state being ^3F in octahedral symmetry. The term ^3F splits as $^3A_{2g}(F)$, $^3T_{2g}(F)$ and $^3T_{1g}(F)$; ^3P as $^3T_{1g}(P)$; ^1D as $^1E_g(D)$ and $T_{2g}(D)$; ^1G as $^1A_{1g}(G)$,$^1T_{1g}(G)$, $^1T_{2g}(G)$ and $^1E_g(G)$; ^1S as $^1A_{1g}(S)$, once a ligand field is introduced.[37] The three spin-allowed transitions are: $^3A_{2g}(F)$ to $^3T_{2g}(F)$; $^3A_{2g}(F)$ to $^3T_{1g}(F)$ and $^3A_{2g}(F)$ to $^3T_{1g}(P)$. The two spin-forbidden transitions are: $^3A_{2g}(F)$ to $^1E_g(D)$ and $^3A_{2g}(F)$ to $^1T_{2g}(D)$. Generally, three intense (spin-allowed) and two weak (spin-forbidden) bands are expected for nickel(II) ions in octahedral configuration.

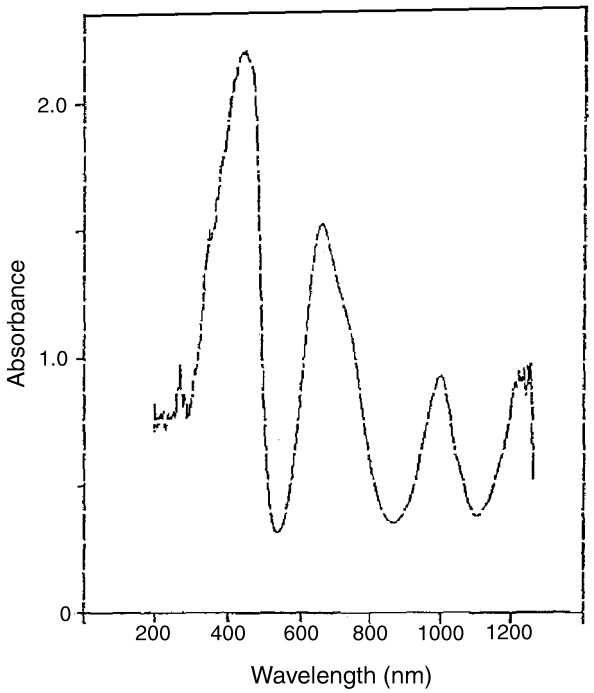

Figure 1. UV-Vis spectrum of the nickel complex in methanol solvent. This spectrum is useful for calculating optical parameters.

The finely powdered sample of the nickel complex is dissolved in ethanol and the spectrum is recorded from 200 to 1300 nm. Figure 1 gives the optical spectrum of the nickel complex. Three strong peaks are observed at 400, 660 and 998 nm and the assignments are:

$$^3A_{2g}(F) \rightarrow {}^3T_{2g}(F),\ 998\ \text{nm} = 10020\ \text{cm}^{-1},$$

$$^3A_{2g}(F) \rightarrow {}^3T_{1g}(F),\ 660\ \text{nm} = 15151\ \text{cm}^{-1},$$

$$^3A_{2g}(F) \rightarrow {}^3T_{1g}(P),\ 400\ \text{nm} = 25000\ \text{cm}^{-1}.$$

A weak band observed at 741 nm is assigned to the forbidden transition, $^3A_{2g}(F)$ to $^1E_g(D)$.

From the normal procedure, the crystal field splitting value (Dq) and the inter electron repulsion parameters B and C (Racah parameters) have been calculated. The final parameters are

$$Dq = 1019\ \text{cm}^{-1} \text{ and } B = 698\ \text{cm}^{-1}.$$

B for a free nickel(II) ion is 1080 cm^{-1}, which indicates a reduction of about 35% from the free ion value. Another weak band, corresponding to the transition from $^3A_{2g}(F)$ to

$^1T_{2g}(D)$, expected at 428 nm (calculated from the theoretical calculations), is not seen in this case due to its very low intensity.

3.3 *Electron paramagnetic resonance*

The preparation of this nickel complex is similar to that of a previously reported copper complex.[33] The frequencies of the IR spectra of copper complex[33] are comparable to those of this nickel complex. As X-ray data of only the copper complex is available and not that of the nickel complex, this close resemblance in IR data is useful to assume similar structures for the copper and nickel complexes. The nickel complex gives a well-resolved EPR spectrum at room temperature, even though it is a d^8 system. Very few d^8 systems that exhibit room temperature EPR spectra are known in the literature. Hence, single crystal rotations are performed in three orthogonal planes and the data are analysed. The results indicate that the complex has very low distortion, indicated by a low value for zero-field splitting. The *g* and *D* matrices have been analysed and compared with the X-ray data of copper complexes.[33] The EPR results further point out that the two nickel ions present in the complex do not interact appreciably to give complicated and broadened spectra. Using the optical data, *Dq* and Racah parameters are calculated, from which the covalency of the metal–ligand bond is estimated. Good single crystals suitable for EPR studies are selected for crystal rotations in the three orthogonal planes. As the X-ray data of the complex is not known, we have no *a priori* knowledge of the structure of the complex and its coordinating system. Hence, a fine single crystal with clearly identifiable axes is chosen. The longest axis of the crystal is chosen as the *a*-axis. The *b*-axis is chosen on a big plane having an *a*-axis and perpendicular to it. The third orthogonal axis is chosen as the *c*-axis. The credibility of the chosen axes is approved after comparing the results of the powder and single crystal work.

The crystal with *ab* plane is mounted on a goniometer for EPR rotations. In this plane, a single line is observed throughout the crystal rotation. However, the resonance lines show *g* anisotropy. This immediately concludes that the zero-field splitting (*D*) is very small in this plane and close to zero. If *D* is not zero, a pair of lines, separated by 2*D*, is expected. On the other hand, if *D* is large, a single line is observed at a position corresponding to one of the two transitions and the *g* value of the line is far away from 2·2. A typical EPR spectrum obtained when the applied magnetic field is parallel to the crystal *b*-axis is shown in figure 2. Crystal rotations are made for every 10° and the isofrequency plot in the *ab* plane is given in figure 3. The crystal is then mounted along the *b* axis, i.e., *ac* plane and the crystal rotations are made. Two such spectra at different orientations are given in figure 4. Here, one notices a splitting of resonance lines, indicating the non-zero value of *D* in this plane. The road map in the *ac* plane is given in figure 5. Figures 6 and 7 respectively correspond to EPR spectra at two different orientations and the roadmap in the *bc* plane. Schonland[34] and EPR-NMR programs[35] are used to obtain the *g* and *D* matrices from the three road maps. The results are given in table 1. Here also, similar to single crystal work done on a copper complex with Hsalamp ligand,[36] the direction cosines of the *g* and *D* tensors do not match well. However, a close look at them indicates that the *g* and *D* are along a particular axis, say *a*, *b* or *c*. This is not so in the case of other copper complexes.[36] In addition, EPR work done on a nickel(II) complex from our laboratory, in which it is doped into a hexaimidazole zinc(II)dichloride tetrahydrate lattice, the *D* tensor behaves very similarly to the present case. Hence, we can say that the choice of our coordinate system is not that bad.

Moreover, powder work, as mentioned below further confirms our results. Table 2 contains spin Hamiltonian data for a few nickel(II) complexes known in literature.

The powder EPR spectrum of the complex recorded at room temperature is shown in figure 8. As the *D* value obtained from single crystal rotation is close to 21 mT, the resolution into two components due to zero field splitting cannot be seen, due to the breadth of the spectrum. Using the program EPR-NMR,[35] the powder spectrum is simulated using the data given in table 1 and the agreement between experimental and theoretical spectra is very good.

However, the presence of two nickel ions, as indicated by elemental analysis could not be confirmed with our EPR studies. One can argue that due to the similar geometric configurations of the two complexes, both give rise to identical spin Hamiltonian parameters. Even if a small difference in spin Hamiltonian parameters exists, it cannot be seen due to the breadth of the EPR resonance lines. Cooling the sample to 77 K does not decrease the line width appreciably. Further confirmation may come if one studies the EPR spectrum at *Q*-band frequencies and if possible at low temperatures. This could not

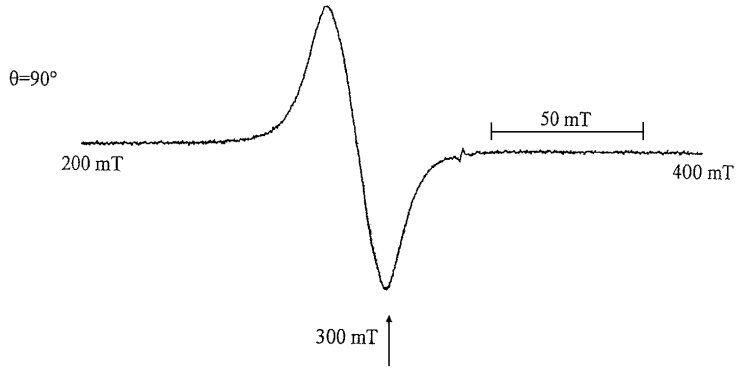

Figure 2. Single crystal X-band EPR spectrum of the nickel complex at room temperature in the *ab* plane. The EPR spectrum corresponds to the orientation when the applied magnetic field (B) is parallel to the crystal *b*-axis. Frequency = 9·09134 GHz.

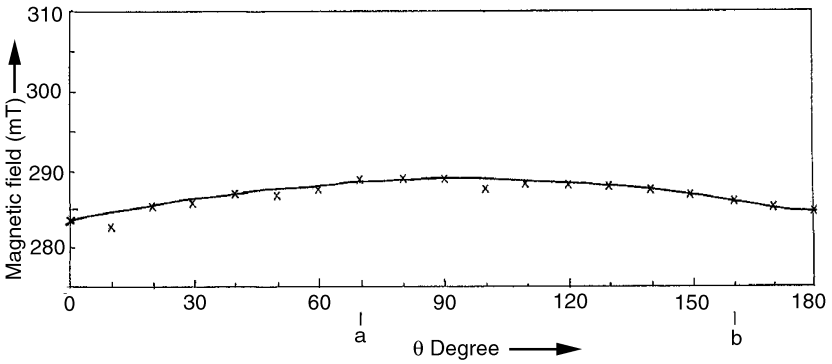

Figure 3. Isofrequency plot in the *ab* plane for nickel(II)/Hsalamp complex at room temperature. Frequency = 9·09134 GHz.

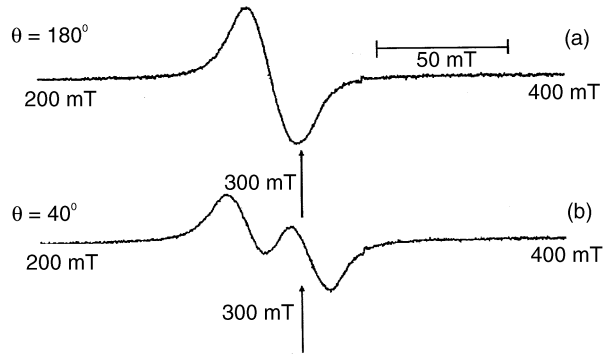

Figure 4. Single crystal X-band EPR spectra of the nickel complex at room temperature in the *ac* plane. The spectra correspond to two orientations (q = 40 and 140°). Frequency = 9·09134 GHz.

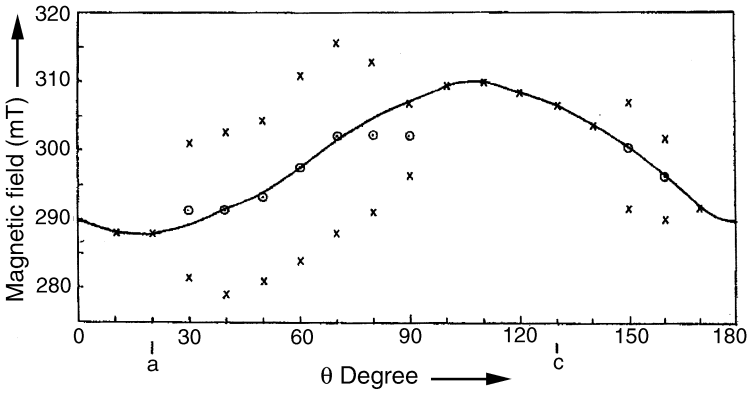

Figure 5. Isofrequency plot in the *ac* plane for nickel(II)/Hsalamp complex at room temperature. Whenever two resonances are noticed, the average is considered for plotting these plots here and in figure 7. Frequency = 9·09134 GHz.

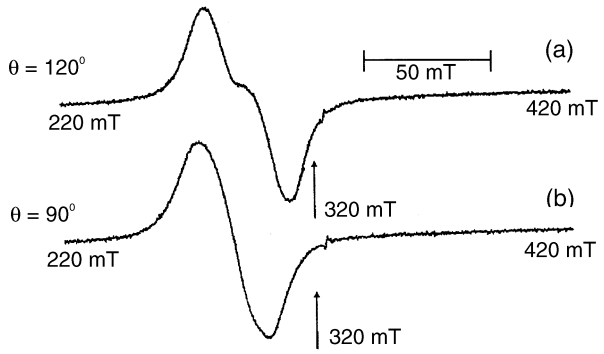

Figures 6. Single crystal X-band EPR spectra of the nickel complex at room temperature in the *bc* plane. These spectra correspond to two orientations (q = 90 and 120°). Frequency = 9·09248 GHz.

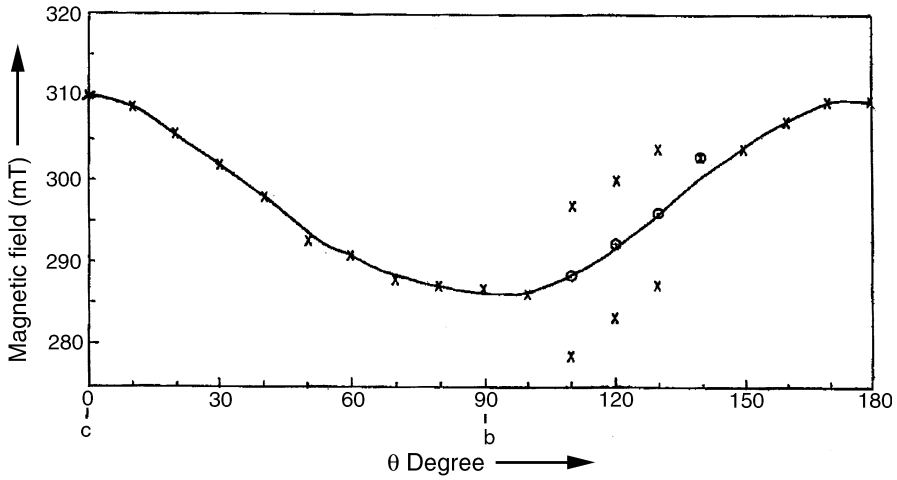

Figure 7. Isofrequency plot in the *bc* plane for nickel(II)/Hsalamp complex at room temperature. Frequency = 9·09248 GHz.

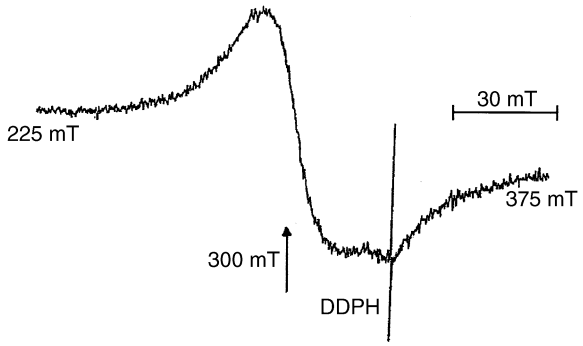

Figure 8. EPR powder spectrum of nickel(II)/Hsalamp complex at room temperature. Since *D* is not large, the two zero-field transitions are merged to give a single broad line (see text). Frequency = 9·41912 GHz.

Table 1. Principal values of *g* and zero-field (*D*) tensors and their direction cosines in an orthorhombic framework.

			Eigenvalues	Eigenvectors		
g matrix						
2·219	−0·008	−0·002	2·377	−0·050	−0·999	−0·007
	2·344	0·094	2·219	0·944	−0·045	−0·327
		2·104	2·071	0·326	−0·023	0·945
D matrix (mT)						
5·45	−0·61	−3·46	9·7	0·531	0·837	−0·129
	−6·43	−10·2	4·2	0·438	−0·402	−0·804
		0·98	−13·9	−0·725	0·370	−0·581

Table 2. Spin Hamiltonian parameters for nickel(II) in a few host lattices.

Host lattice	*g* values	*D* (mT)	Ref.
NHIN*	2·185	882·0	23
NFHH	2·229, 2·261	–129·8	24
Al_2O_3	2·1948, 2·1853	–1·312	25, 26
$RbCaF_3$	2·30, 2·29, 2·32, 2·32	30·7**, 9·9**	28
HZDT	2·3691, 2·2105, 1·9405	244·07, 24·98, – 269·05	22
Ni complex	2·377, 2·219, 2·071	9·7, 4·2, – 13·9	Present study

*Abbreciations: NHIN – nickel hexaimidazole nitrate; NFHH – nickel fluoroborate hexahydrate; HPZ – hexakis pyrazole zinc(II); HPC – hexakis pyrazole cadmium(II); HZDT – hexaimidazole zinc(II)dichloride tetrahydrate
**In units of GHz, two phases at 25 K

be done due to lack of facilities at our centre. Moreover, if the two nickel atoms interact, one would expect the total spin to be 2 and, hence, needs very low temperatures to observe the EPR spectrum. Hence, the suggestion of interaction between the two nickel ions is ruled out, even though the distance between them is comparable to that of copper atoms (assuming identical structures for copper and nickel complexes, Cu–Cu distance is 2·8324 Å). In the case of copper, the proper overlapping of orbitals is permitted resulting in an exchange interaction, which is not so in the case of nickel complexes. Hence, further work at *Q*-band frequencies followed by single crystal X-ray work will really help to completely understand the system.

The optical and EPR data are correlated and the individual spin orbital coupling parameter (l) is calculated using the formula

$$g = 2{\cdot}0023 - 8l/\Delta.$$

The value of l obtained is 280 cm^{-1}, while the free nickel(II) ion value is 324 cm^{-1}. A reduction of 14% is obtained, which corresponds to the percentage of covalent bonding. It is slightly higher than the corresponding values in the Ni(II)–imidazole,[23] Mn(II)–imidazole[38] and Cu(II)–imidazole[39] bonds. The total spin-orbit coupling parameter (x) is calculated using the formula

$$l = \pm x/2S \ (S = 1 \text{ for Ni(II)}),$$

$$x = -560 \text{ cm}^{-1},$$

here the positive sign is required for a shell that is less than half-filled and the negative sign for a shell that is more than half-filled.

The Racah parameters B and C are also calculated theoretically by using the equations below:

$^3A_{2g}(F)$	0
$^3T_{2g}(F)$	$10Dq$
$^3T_{1g}(F)$	$1/2[(15B + 30Dq) - ((9B - 10Dq)^2 + 144B^2)^{1/2}]$
$^1E_g(D)$	$1/2[(17B + 4C + 20Dq) - ((B + 20Dq)^2 + 48B^2)^{1/2}]$
$^1T_{2g}(D)$	$1/2[(17B + 4C + 30Dq) - ((B + 10Dq)^2 + 48B^2)^{1/2}]$
$^3T_{1g}(P)$	$1/2[(15B + 30Dq) + ((9B - 10Dq)^2 + 144B^2)^{1/2}]$

The B value obtained from the above is 640 cm^{-1}, close to the B value obtained by using the Tanabe–Sugano diagram. The calculated C value is 4202 cm^{-1}. The B'/B and C'/C values are 0·62 and 0·86 respectively and are not very close due to interaction with the other nickel atom. These ratios are expected to be close, since reduction should be the same whether the transition is between states of same spine multiplicity or different multiplicity. Here B' and C' are inter-electron repulsion parameters for free nickel(II) ion. From the optical results, one can say that the symmetry around the metal ion is nearly octahedral on this time scale. However, on the EPR time scale the symmetry is proved to be orthorhombic, as mentioned earlier.

4. Conclusion

The synthesis of a binuclear nickel(II) complex is achieved. The complex is characterized by various techniques, which confirm the expected structure for the complex. Interestingly, the EPR data are observable even at room temperatures, making it one of the very few systems giving rise to EPR resonances at room temperature. The spin Hamiltonian parameters have been calculated from single crystal data. The distortion is small and the interaction between the two nickel centres is also very weak. Further work at *Q*-band frequencies and single crystal X-ray work will help to understand the system in a more detailed way.

Acknowledgements

The authors thank the University Grants Commission, the Council of Scientific & Industrial Research, All India Council of Technical Education and the Department of Science & Technology for financial assistance.

References

1. West D X, Liberta A E, Padhye S B, Chikate P B, Sonawane A S, Kumbhar O and Yerande R G 1993 *Coord. Chem. Rev*. **123** 49
2. Kovala-Demertzi D, Domopoulou A, Demertzis M, Raptopoulou C and Terzis A 1994 *Polyhedron* **13** 1917
3. West D X, Lockwood M S and Castineiras A 1997 *Transition Met. Chem*. **22** 447
4. West D X, Gebremedhin H, Butcher R J and Jasinski J P 1995 *Transition Met. Chem*. **20** 84
5. Kovala-Demertzi D, Domopoulou A, Demertzis M A, Valle G and Papageorgiou A 1997 *J. Inorg. Biochem*. **68** 147
6. Di Vaira M, Orioli P L and Sacooni L 1971 *Inorg. Chem*. **10** 553
7. Seleborg M, Holt S L and Post B 1971 *Inorg. Chem*. **10** 1501
8. Healy P C, Mockler G M, Freyberg D P and Sinn E 1975 *J. Chem. Soc., Dalton Trans*. 691
9. Freyberg D P, Mockler G M and Sinn E 1976 *J. Chem. Soc., Dalton Trans*. 447
10. Sczaniecki P B and Lesiak J 1982 *J. Magn. Reson*. **46** 185
11. Sano W, Domiciano J B and Ochi J A 1994 *Phys. Rev*. **50** 5
12. Kadish K M, Sazou D, Maiya G B, Han D C, Sasiabi A, Ferhat M and Guilard R 1989 *Inorg. Chem*. **28** 2542
13. Bencini, Alessandro, Farbrizzi, Luigi, Poggi and Antonio 1981 *Inorg. Chem*. **20** 2544
14. Bencini A, Gatteschi D and Sacconi L 1978 *Inorg. Chem*. **17** 2768
15. Rubins R S and Yung Y H 1981 *J. Chem. Phys*. **75** 4285
16. Rubins R S and Haghighatojou T 1982 *J. Phys. Chem. Solids* **43** 491
17. Zhao M G, Du M L and Sen G Y 1987 *J. Phys. Chem. Solid State Phys*. **33** 5557

18. Shrivastava K N, Rubenacker G N, Hutton S L, Drumheller J E and Rubins R S 1988 *J. Chem. Phys*. **88** 634
19. Shrivastava K N, Hutton S L, Drumheller J E and Rubins R S 1988 *J. Chem. Phys*. **88** 705
20. Shreerama Chandra Prasad L and Subramanian S 1988 *J. Chem. Phys*. **43** 88
21. Rammu S, Lahmann G, Recker K and Wallrafen F 1986 *Z. Naturforsch*. **A41** 619
22. Griffith J H E and Owen J 1952 *Proc. R. Soc.* **A213** 459
23. Velavan K, Rajendiran T M, Venkatesan R and Sambasiva Rao P 2002 *Solid State Commun.* **15** 122
24. Lochar P R and Geschwind S 1963 *Phys. Rev. Lett*. **11** 333
25. Marshell S A, Kikuchi T T and Reinberg A R 1962 *Phys. Rev*. **125** 453
26. Xavier Anthonisamy V S, Padiyan D P and Murugesan R 1998 *Mol. Phys*. **94** 275
27. Lahoz F, Villacampa B and Alcala R 1997 *J. Phys. Chem. Solids* **58** 881
28. Socrates G B 2001 *Infrared and Raman spectral frequencies* 3rd edn (New York: John Wiley & Sons)
29. Gupta R, Mukherjee S and Mukherjee R 1999 *J. Chem. Soc., Dalton Trans*. 4025
30. Rosenthal M R 1973 *J. Chem. Edu*. **50** 331
31. Geary W J 1971 *Coord. Chem. Rev*. **7** 81
32. Boge E M, Freyberg D P, Kokot E, Mockler G M and Sinn E 1977 *Inorg. Chem*. **16** 1655
33. Srinivasan R, Venkatesan R, Rajendiran T M and Sambasiva Rao P (to be submitted)
34. Schonland D 1959 *Proc. Phys. Soc*. **73** 788
35. Program developed by Clark F, Dickson R S, Fulton D B, Isoya J, Lent A, McGavin D G, Mombourquette M J, Nuttall R H D, Rao P S, Rinneberg H, Tennant W C and Weil J A, University of Saskatchewan, Saskatoon, Canada, 1996
36. Srinivasan R, Venkatesan R, Rajendiran T M and Sambasiva Rao P (to be submitted)
37. Figgis B N 1966 *Introduction to ligand fields* (New Delhi: Wiley Eastern)
38. Sambasiva Rao P and Subramanian S 1985 *Mol. Phys*. **54** 429
39. Sambasiva Rao P and Subramanian S 1976 *J. Magn. Reson.* **22** 191